Electronic Supporting Information

Asymmetric triply bridged lanthanide binuclear clusters with distinctly different magnetic behaviors

Yue Yang,[a] Yu-Xia Wang,[a,b]* Yu-Zhe Lei,[a] Peng Cheng[a]*

[a] Department of Chemistry, Key Laboratory of Advanced Energy Materia Chemistry, Frontiers Science Center for New Organic Matter, and Haihe Laboratory of Sustainable Chemical Transformations (Tianjin), College of Chemistry, Nankai University, Tianjin 300071, China.

[b] Tianjin Key Laboratory of Structure and Performance for Functional Molecules, College of Chemistry, Tianjin Normal University, Tianjin 300387, P. R. China Nankai University, Tianjin 300071, China.

*Corresponding authors:

E-mail: (wangyuxiank@163.com; pcheng@nankai.edu.cn)

1. Physical measurements

All materials of the chemicals and solvent reagents are obtained commercially and used in reactions without further purification. Thermogravimetric analysis (TGA) was carried out using a NETZSCH TG 209F3 analyzer. Fourier transform infrared (FTIR) spectra were recorded on a Thermo Scientific Nicolet iS10 spectrophotometer in the range of 400-4000 cm^{-1}. Powder X-ray diffraction (P-XRD) was measured using the Rigaxu Ultima-VI X-ray diffractometer. The measurements of magnetic properties were performed on the Quantum Design MPMS-XL7 ($\chi_M T$-T) and Quantum Design PPMS-VSM. Both the diamagnetic contribution of the sample holder and the diamagnetism estimated using Pascal's constants were corrected.

2. Syntheses

The **Dy** samples were synthesized by solvothermal reaction. $Dy(NO_3)_3 \cdot 6H_2O$ (0.5 mmol, 228.3 mg) was slowly added to a 15 mL ethanol solution containing H_4L (1.0 mmol, 236.3 mg) and PhCOOH (1.5 mmol, 183.2 mg). The mixture was moved to a vial after 0.5 h of stirring. Colorless crystals were obtained under 90 ˚C solvothermal condition three hours later in a 56% yield (based on Dy). The synthesis method of **Gd** is the same as that of **Dy**, only $Dy(NO_3)_3 \cdot 6H_2O$ needs to be replaced with $Gd(NO_3)_3 \cdot 6H_2O$, the crystal color is colorless, and the yield is 41% based on Gd.

3. X-Ray crystallography

Single-crystal X-ray data of **Dy** and **Gd** were collected at 120 K on a Rigaku XtaLAB Synergy R, HyPix High-Flux Rotating Anode X-ray Diffractometer equipped with graphite-monochromated Cu-Kα radiation (λ = 1.54184 Å). The structures were solved employing direct methods and refined employing the full-matrix least-squares method on F^2 with anisotropic thermal parameters for all nonhydrogen atoms. Hydrogen atoms were added geometrically and refined using a riding model. CCDC: 2383322 and 2383323.

4. Structural complement

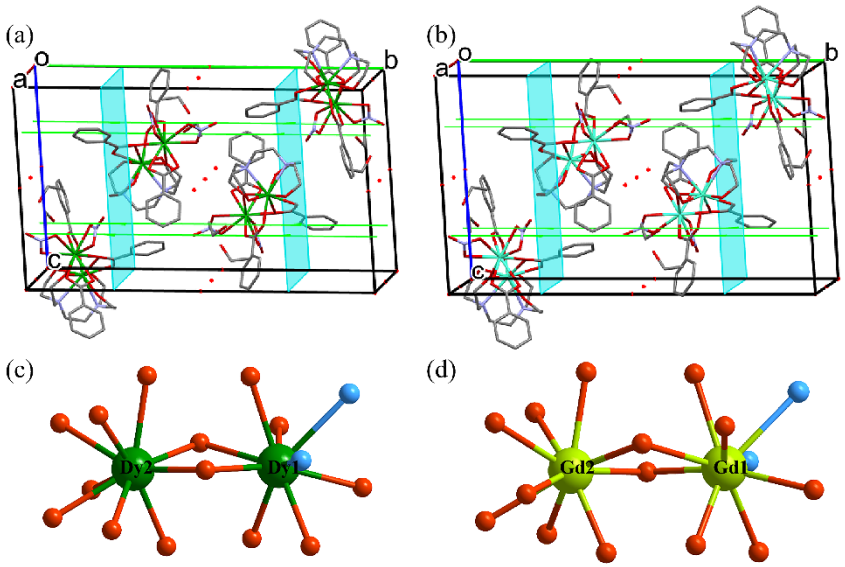

Fig. S1 Symmetrical elements of **Dy** (a) and **Gd** (b). The blue-green planes represent the glide planes parallel to the (010), the green lines represent the 2_1-screw axes (b-axes), and the red dots represent the inversion centers. Coordination environment of **Dy** (c) and **Gd** (d), red atoms, O; blue atoms, N.

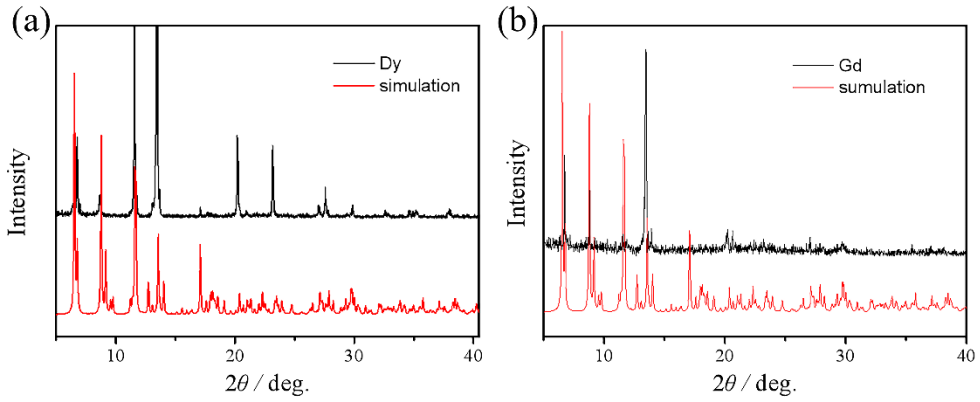

Fig. S2 Powder-XRD patterns of **Dy** (a) and **Gd** (b), the black lines are the experimental values and the red lines are the simulated values.

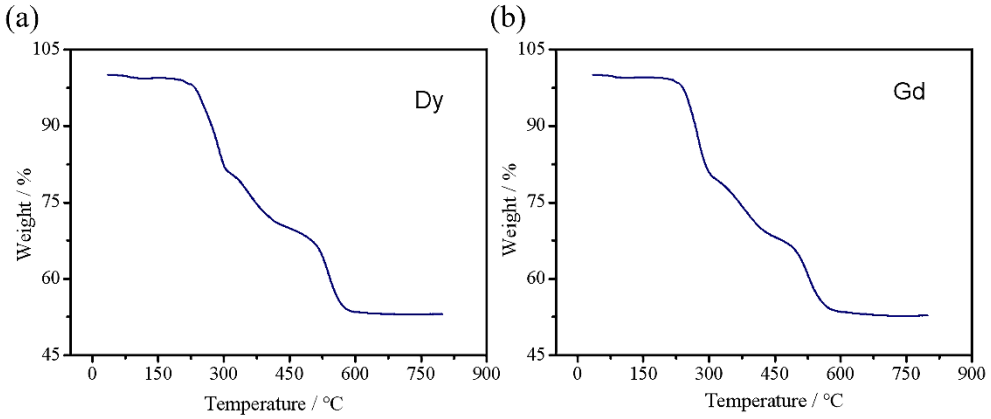

Fig. S3 TG curves of **Dy** (a) and **Gd** (b).

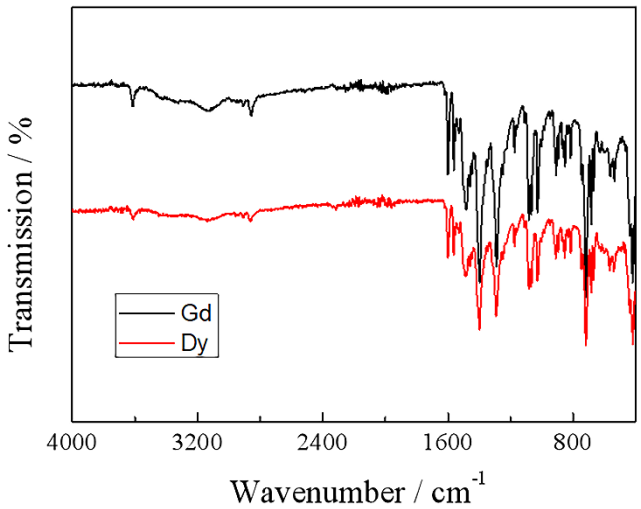

Fig. S4 Infrared spectral data of **Dy** and **Gd**. The black and red lines represent **Dy** and **Gd**, respectively.

5. Magnetic characterization

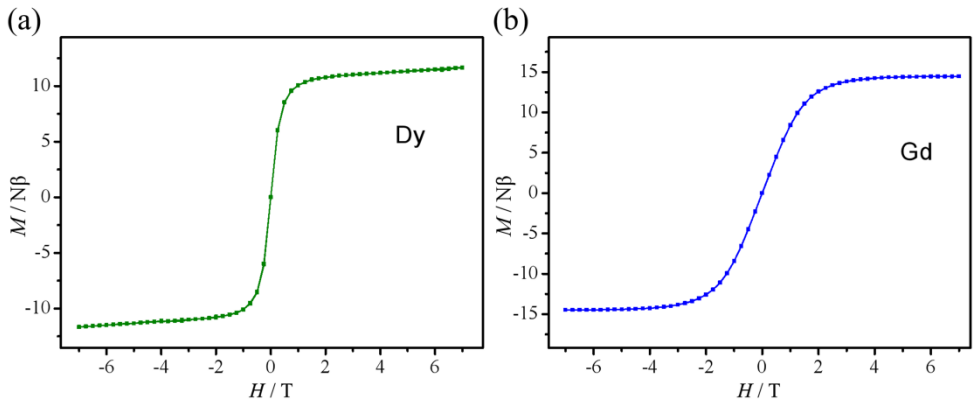

Fig. S5 Magnetic hysteresis of **Dy** (a) and **Gd** (b) at 2 K.

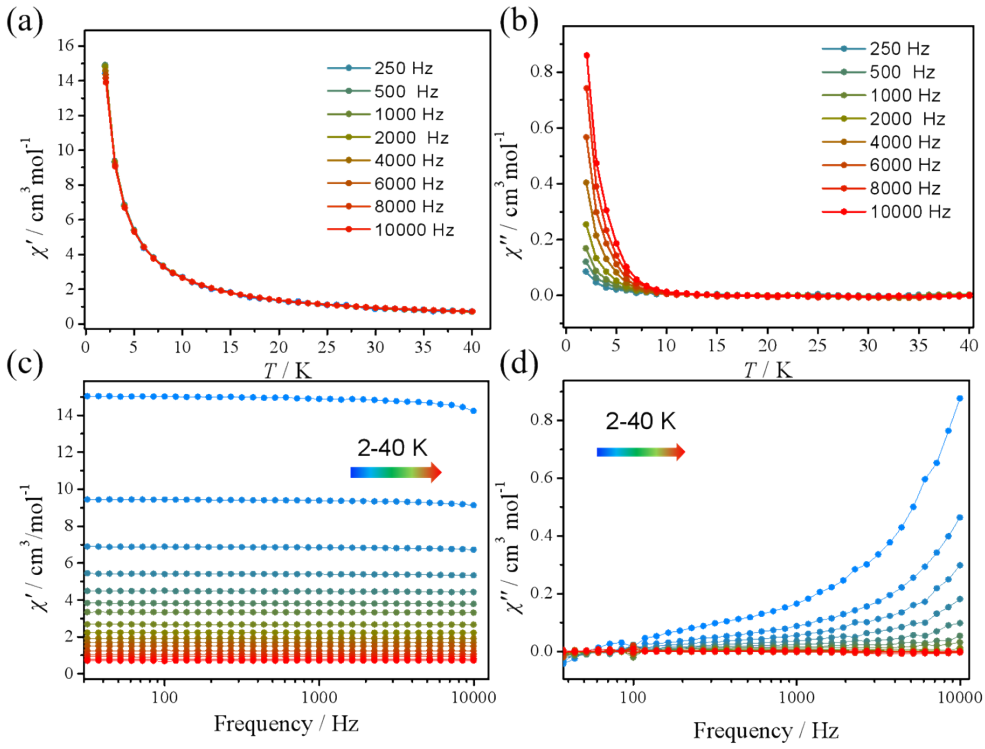

Fig. S6 Ac molar magnetic susceptibility measurements of **Dy**. Temperature (a, b) and frequency (c, d) of the in-phase χ' and out-of-phase χ'' products under a 0 Oe dc field in the temperature range of 2-40 K. Solid lines are guides for the eyes.

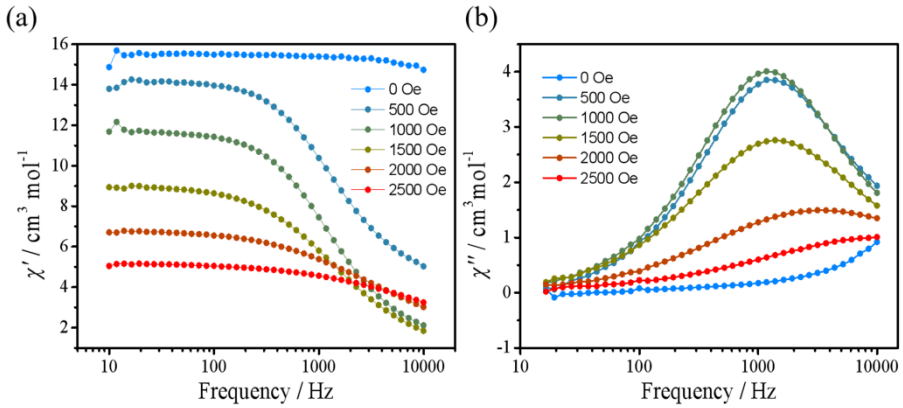

Fig. S7 Alternating-current molar magnetic susceptibility measurements. Frequency dependence of the in-phase χ' (a) and out-of-phase χ'' (b) products under varying applied dc fields (0-2500 Oe) at 2 K of **Dy**. Solid lines are guides for the eyes.

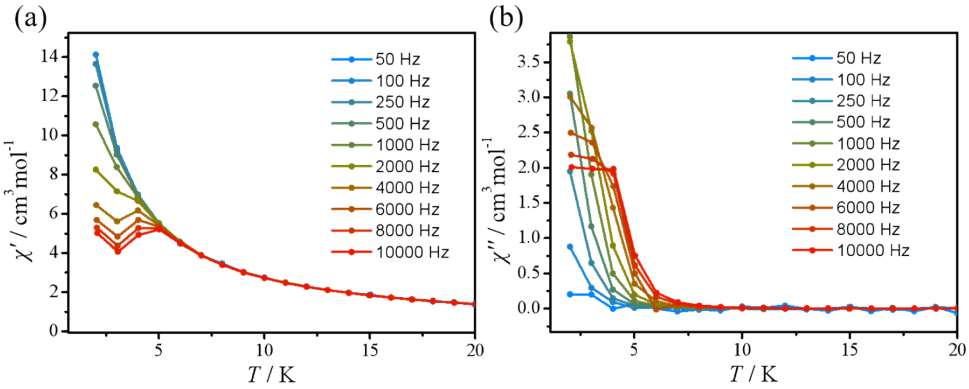

Fig. S8 Temperature dependence of the in-phase (χ') and out-of-phase (χ'') ac molar susceptibilities measured on a polycrystalline sample under the 500 Oe field of **Dy**. Solid lines are guides for the eyes.

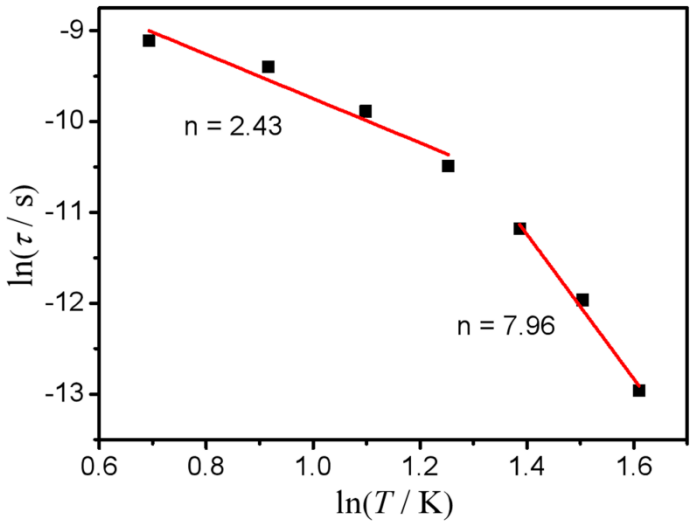

Fig. S9 Plots of ln(*T*) *vs*. ln(τ); solid red lines represent the best linear fits.

6. Table

Table S1 A part of crystallographic parameters of **Dy** and **Gd**.

Compound	**Dy**	**Gd**
Formular	$[Dy_2(PhCOO)_3(H_3L)(NO_3)_2]\cdot 2C_2H_5OH$	$[Gd_2(PhCOO)_3(H_3L)(NO_3)_2]\cdot 2C_2H_5OH$
T (K)	120	120
Space group	$P2_1/n$	$P2_1/n$
a (Å)	10.27550(10)	10.3156(2)
b (Å)	26.0316(2)	26.0237(4)
c (Å)	16.4282(2)	16.4697(2)
$\alpha = \gamma$ (deg.)	90	90
β (deg.)	105.8520(10)	105.754(2)
V(Å^3)	4227.23(8)	4255.21(12)
Z	4	4
Dc (g·cm^{-3})	1.791	1.763
μ (mm^{-1})	19.374	20.619
R_{int}	0.0397	0.0547
GOOF	1.072	1.088
R_1	0.0440	0.0463
wR_2	0.0944	0.1032
$\triangle\rho_{max}$ (e Å^{-3})	1.35	1.67
$\triangle\rho_{min}$ (e Å^{-3})	-1.20	-1.26

Table S2 Continuous shape measure calculations for the Dy^{3+} ions.

Dy			
Dy1			
[ML9]	JCSAPR-9	CSAPR-9	MFF-9
Shape	C_{4v}	C_{4v}	C_s
Symmetry	Capped square antiprism J10	Spherical capped square antiprism	Muffin
Deviation value	2.409	2.220	2.495
Dy2			
[ML9]	CSAPR-9	TCTPR-9	MFF-9
Shape	C_{4v}	D_{3h}	C_s
Symmetry	Spherical capped square antiprism	Spherical tricapped trigonal prism	Muffin
Deviation value	2.132	2.449	2.399

Table S3 Continuous shape measure calculations for the Gd^{3+} ions.

Gd			
Gd1			
[ML9]	JCSAPR-9	CSAPR-9	MFF-9
Shape	C_{4v}	C_{4v}	C_s
Symmetry	Capped square antiprism J10	Spherical capped square antiprism	Muffin
Deviation value	2.549	2.331	2.577
Gd 2			
[ML9]	CSAPR-9	TCTPR-9	MFF-9
Shape	C_{4v}	D_{3h}	C_s
Symmetry	Spherical capped square antiprism	Spherical tricapped trigonal prism	Muffin
Deviation value	2.334	2.569	2.575

Table S4 The –Δ*S*m for selected dinuclear Gd_2 clusters.

Binuclear Gd compounds	$-\Delta S_m$ (J kg^{-1} K^{-1})	T (K)	ΔH (T)	Ref.
$[Gd_2L_4(CH_3COO)_2(CH_3OH)_2]$	39	2	7	43
$[Gd_2(PhCOO)_3(H_3L)(NO_3)_2]\cdot 2C_2H_5OH$	32.37	2	14	This work
$[Gd_2(PhCOO)_3(H_3L)(NO_3)_2]\cdot 2C_2H_5OH$	29.44	2	7	This work
$[Gd_2(iba)_6(bipy)_2]$	29.3	2	7	44
$[Gd_2(nic)_6(H2O)_4]$	27.4	2.5	7	44
$[Gd_2(H_3L)_2(NO_3)_2](NO_3)_2$	27.50	2	7	22
$[Gd_2(OAc)_2(Ph_2acac)_4(MeOH)_2]$	23.7	2.4	7	45
$[Gd_2(HFAC)_4(L1)_2]$	17.66	2	7	46
$[Gd_2(HFAC)_4(L2)_2]$	14.81	3	7	46
$[Gd_2(tfac)_4(L)_2]$	23.23	2	8	47
$[Gd_2(hfac)_4(L)_2]$	17.05	2	8	47

Table S5 Cole-Cole plot fitting parameters for **Dy** in an external field of 500 Oe.

T (K)	χ_s (cm^3 mol^{-1})	χ_t (cm^3 mol^{-1})	τ (s)	α
2	3.94532	13.4081	1.10283E-4	0.16
2.5	3.22475	10.589	8.26235E-5	0.14343
3	2.68273	8.71643	5.08463E-5	0.13387
3.5	2.32571	7.39668	2.778E-5	0.12061
4	2.07328	6.41588	1.39235E-5	0.10181
4.5	1.74928	5.672	6.35897E-6	0.10524
5	0.95711	5.08107	2.34359E-6	0.13564

Table S6 The best fitting results of the temperature dependent relaxation times.

$\tau^{-1} = AHT + \tau_{QTM}^{-1} + CT^n + \tau_0^{-1} \exp(-U_{eff}/k_BT)$	
AH	4292.01
B	0.67518
n	8.20481
τ_0	---
U_{eff} (cm^{-1})	---
dominated relaxation processes	Direct + Raman